The Calibration Index and the Role of Input Noise in Robot Calibration

†John M. Hollerbach and ‡Charles W. Wampler
†Dept. Computer Science, Univ. Utah, Salt Lake City, UT 84112
‡Mathematics Dept., General Motors Research and Development, Box 9055, Warren, MI 48090

1 Introduction

This paper addresses two topics in robot calibration: the formulation of a calibration index and the presence of input noise. The calibration index is introduced to succinctly capture the essence of a kinematic calibration method and allow insightful comparison between that method and other methods. Input noise, e.g., joint angle errors, is a potential source of error that is usually ignored, but is known to lead to bias errors in the estimates (Norton 1986). The two topics also will be seen to have a relationship.

Many kinematic calibration methods have been proposed by now, and more are continually introduced. These methods differ in terms of whether an external metrology system is required (open-loop methods) or not (closed-loop methods), how many components of pose are measured and by what means, how many components of pose are passively constrained and how, whether there are unsensed joints, and whether a serial or parallel mechanism is being calibrated (Hollerbach 1993). It can be very difficult to understand how one method is related to another method, or what the tradeoffs are in selecting a calibration method. This statement is particularly true for parallel linkages, with different mixtures of sensed and unsensed joints, and passive and active joints. It is not always immediately obvious how easy a parallel linkage is to calibrate, especially by a closed-loop method.

The literature on camera calibration is usually distinct from that on manipulator calibration. By modeling cameras and light beams as prismatic legs, it is possible to fold camera calibration into manipulator calibration. An advantage is that mixed manipulator/camera calibration problems can be handled uniformly.

2 Closed-Loop Viewpoint

An enabling step to clarify this picture was suggested in (Wampler and Arai, 1992; Hollerbach 1993; Wampler et al. 1995): nearly all kinematic calibration approaches can be viewed as closed-loop approaches, where the end effector measurement in open-loop methods is considered to form a joint. All measurements, whether from joints or metrology systems, are put on an equal footing, as are all unsensed joints, whether from unsensed components of pose, passive environmental constraints, or joints in the chain without sensors. In the case of parallel linkages, sufficient numbers of loop closure equations are formulated to characterize the kinematics and are combined at each pose.

Figure 1 illustrates this idea for a calibrated stereo camera metrology system that measures the 3D coordinates of a distinguished point on the end effector of an uncalibrated robot. On the right this camera system has been replaced by a prismatic leg, which stylistically represents a 6-DOF joint that provides equivalent 3D coordinate measurements. The result is a closed-loop mechanism.

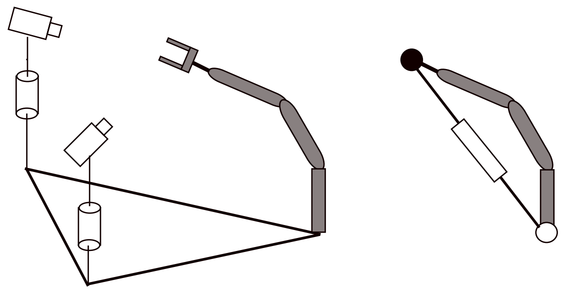

Figure 1: External metrology system modeled as a 6-DOF joint.

2.1 Uncalibrated Visual Sensors

As suggested in the Introduction, visual sensors can be modeled as prismatic legs. In the case of a laser interferometer, the laser beam is typically scanned by pan-tilt mirrors to a retroreflector on the endpoint, and can be modeled as a Hooke joint (pan-tilt mirror), followed by a sensed prismatic joint (the beam length measured interferometrically), and ending with a spherical joint (reflection from the retroreflector). Thus a scanning laser interferometer can be viewed very much as a 6-DOF leg on a Stewart platform or other parallel-drive platform (Figure 2).

Figure 2: A camera and light beam modeled as prismatic leg (box), with hook joint (open circle) and spherical joint (solid circle) at either end.

In the case of a camera, the detector tracks a fixed distinguished point in the environment. The light ray from the camera to the tracked point is also modeled as a prismatic leg. The fixation point on the end effector is modeled as forming a spherical joint with the light ray. The detector measures in terms of linear image coordinates, and can be stylized also as a Hooke joint located at the lens focal point. The scenario of Figure 1 can now be replaced with Figure 3, where the stereo camera system as well as the manipulator are uncalibrated, and both can be calibrated together (Bennett et al. 1991).

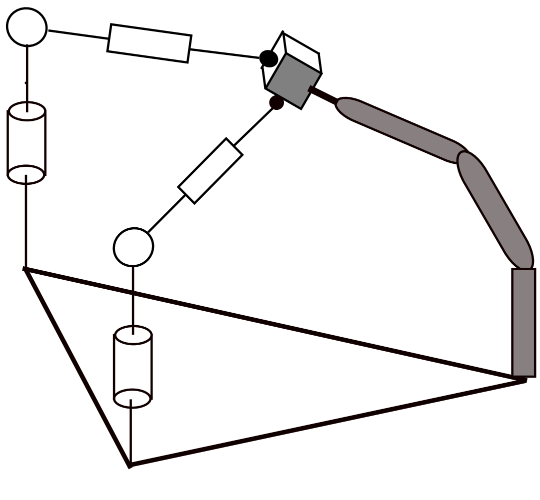

Figure 3: Mechanical equivalent of a stereo camera system on single-DOF tripods tracking a point on a 6-DOF arm.

In manipulator calibration, we distinguish between geometric parameters, such as the Denavit-Hartenberg parameters, and non-geometric parameters, which typically are confined to a joint and express some functional relation between the true joint angles and the joint angle measurements. Nongeometric parameters include joint angle gains, joint angle offsets, and gear eccentricities (Whitney et al., 1986). Similarly, lens and detector parameters for a camera, such as focal length, offsets between the image plane readings and the optical center (Bennett et al. 1991), and radial lens distortion (Zhuang et al. 1995) are analogous camera nongeometric parameters that can be calibrated.

2.2 Loop Closure Equations

Assume the robot is placed into p poses. Following the formulation in (Hollerbach 1993; Wampler et al. 1995), all kinematic calibration methods are considered as closed-loop methods, wherein any endpoint measurement system is considered to form a joint. Consequently, form the kinematic loop closure equations $\mathbf{f}^i$ for the ith pose $(i = 1, ..., p)$:

$$\mathbf{f}^i(\mathbf{x}^i, \boldsymbol{\phi}) = \mathbf{0} \tag{1}$$

where $\boldsymbol{\phi}$ is a vector of robot parameters to be calibrated, and $\mathbf{x}^i$ is a vector of joint sensor readings and possibly external sensor readings. Combine (1) for the p poses into a single matrix equation:

$$\mathbf{f}(\boldsymbol{\phi}) = [\mathbf{f}^{1^T} \dots \mathbf{f}^{p^T}]^T = \mathbf{0} \tag{2}$$

In (2), we treat the sensor readings $\mathbf{x}^i$ as constants for each pose i. Linearize (2) around the nominal values of the parameters:

$$\Delta\mathbf{f} = \frac{\partial \mathbf{f}}{\partial \boldsymbol{\phi}} \Delta\boldsymbol{\phi} = \mathbf{J}\Delta\boldsymbol{\phi} \tag{3}$$

where $\Delta\mathbf{f}$ is the deviation of the computed loop closure equations from zero, $\mathbf{J}$ is the identification Jacobian, and $\boldsymbol{\Delta\phi}$ is the correction to be applied to the current parameter estimate. The calibration problem is then solved by minimizing $\Delta\mathbf{f}$ via iterative least squares.

3 The Calibration Index

3.1 The Mobility Index

With all calibration methods viewed as closed-loop methods, we apply the mobility equation to characterize the degrees of freedom in any calibration setup. The mobility index is (McCarthy 1990):

$$M = 6(L-1) - \sum_{i=1}^{J} D_i \tag{4}$$

where $M =$ mobility index,
$L =$ number of links,
$J =$ number of joints, and
$D_i =$ number of constraints at joint i.

L includes the base link and any extra links attached to the robot to constrain or measure its motion. J includes joints of any additional linkages added for calibration. For a rotational or prismatic joint $D_i = 5$, while for a ball or spherical joint $D_i = 3$. For an external measurement system for a freely moving end effector $D_J = 0$, while for rigid attachment of the endpoint $D_J = 6$.

While (4) is generally correct, there are exceptions due to special or to degenerate mechanisms. The mobility index for planar mechanisms and spherical mechanisms is discussed in (McCarthy 1990). Immobile joints may arise in special cases, such as the immobile elbow joint in anthropomorphic manipulators with fixed end link (Bennett and Hollerbach, 1991). The analysis of special or degenerate mechanisms has to take place on a case-by-case basis, and is best done by looking for linear dependence in the columns of the Jacobian matrix (3). This would happen automatically when checking observability, which reveals any ill conditioning of the Jacobian matrix (Mooring et al., 1991).

3.2 The Sensor Index

The total number of sensors S in the joints can be written as:

$$S = \sum_{i=1}^{J} S_i \tag{5}$$

where $S_i =$ the number of sensed degrees in joint i. We impose the restriction $S_i \leq 6 - D_i$, i.e., there cannot be more sensors than degrees of freedom at a joint. Usually $S_i = 1$ for the lower-order pairs typical of actuated joints, while $S_J = 6$ for full pose measurement of the end effector "joint" J. For an unsensed joint, such as in passive environment kinematics, $S_i = 0$.

3.3 The Calibration Index

Calibration can proceed if $S > M$, that is to say, there is redundant sensing with regard to positioning of the chain. The excess of sensed joints over mobility represents the number of equations per pose that can be used for calibration:

$$C = S - M \tag{6}$$

where we term C the *calibration index.* If P is the number of poses, then CP is the total number of equations for the calibration procedure. Clearly a larger C means less poses are required, other things being equal.

For the single-loop case consisting of a series of sensed lower-order robot joints ($S_i = 1, D_i = 5, \quad i = 1, \ldots, J-1$) with a final joint ($S_J, D_J$) connecting the end-effector to ground, one has from Eqs. (4-6):

$$C = S_J + D_J \tag{7}$$

According to the calibration index, using full endpoint constraints is an equivalent kinematic calibration method to using full pose measurements. There is potentially a problem with smaller pose selection available with endpoint constrained, but otherwise the mathematics are the same.

4 Legs and Limbs

We are now in a position to compare and contrast calibration methods that have appeared in the literature. We can also readily conceive new calibration methods, by picking a calibration index and posing appropriate endpoint measurements or constraints. We now give examples for different values of the calibration index C.

4.1 Metal Limbs

4.1.1 *Serial-Link Manipulators*

All manners of pose measurement and endpoint constraints have been proposed that result in different calibration indices. Existing methods almost never mix measurements and constraints and choose one or the other exclusively. Examples are given for each value of calibration index.

C=6: $D_J = 0$ and $S_J = 6$ corresponds to full pose measurement (e.g., Vincze et al. 1994).

$D_J = 6$ and $S_J = 0$ corresponds to rigid endpoint attachment (Bennett and Hollerbach 1991).

C=5: $D_J = 0$ and $S_J = 5$ corresponds to 5-DOF pose measurement (e.g., Lau et al. 1985).

$D_J = 5$ and $S_J = 0$ corresponds to 5-DOF endpoint constraints, such as manipulation of an unsensed passive hinge joint (Giugovaz and Hollerbach 1994).

C=4: There is a glaring hole here: no published methods exist for $C = 4$ for serial link manipulators! We will fix this lapse of the field. Let's choose $S_J = 0$ and $D_J = 4$, i.e., a closed-loop method with 4 endpoint constraints. Motion along a line with orientation constraint leaves 4 equations per pose: we can rotate about the axis of the line, but not about the other directions. An example is placing a round peg into a round hole. Another example is sliding a door along its hinges.

C=3: $D_J = 0$ and $S_J = 3$ corresponds to 3-DOF pose measurement, which is provided by basic triangulation systems or CMMs (coordinate measuring machines) (Renders et al., 1991).

$D_J = 3$ and $S_J = 0$ corresponds to 3-DOF endpoint constraints, such as fixed point contact (Bennett and Hollerbach 1991; Craig 1993).

C=2: $D_J = 0$ and $S_J = 2$ corresponds to 2-DOF pose measurements, such as is provided by a single theodolite (Whitney et al., 1986).

$D_J = 2$ and $S_J = 0$ corresponds to 2-DOF endpoint constraints. Motion along a line provides two constraints (Newman and Osborn, 1993). This is contrasted to the case for $C = 4$ in that now there is no orientation constraint. Tracking an edge with a stylus is one example; this case is considered more fully in Section 4.2. Motion along a line is just one example of a path constraint on a plane. Actually, tracing any known curve will do, such as a circle.

C=1: $D_J = 0$ and $S_J = 1$ corresponds to measurement of just 1-DOF pose, provided by a linear transducer such as an LVDT or wire potentiometer (Driels 1993). This is like using a single measuring tape.

$D_J = 1$ and $S_J = 0$ corresponds to plane constraint (Zhong and Lewis 1995). Touching a probe anywhere on a plane yields a viable closed-loop approach.

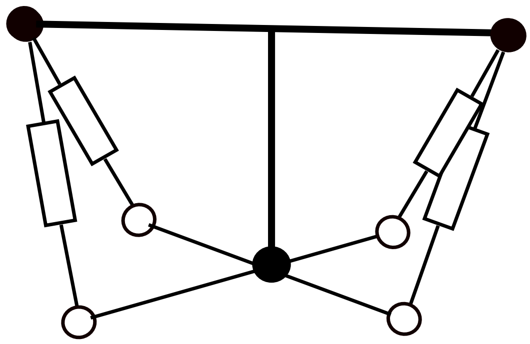

Figure 4: Redundant parallel drive shoulder joint.

4.1.2 *Parallel-Link Manipulators*

Calibration procedures have been increasingly applied to parallel-drive linkages. Often these linkages are platforms activated by prismatic legs (Figure 2), which have a sensed prismatic joint in the middle. Six-DOF rotary legs (i.e., manipulator arms) are also used. The number of legs varies.

Wampler et al. (1995) calibrated the 6-legged Stewart platform ($M = 6$) via a closed-loop procedure. In addition to leg length measurements, all angles on one of the legs were measured ($S = 11$). Hence $C = 5$, and Wampler et al. (1995) were able to forgo an external measurement system. For a regular Stewart platform without the instrumented leg, $S = 6$ and hence $C = 0$. External pose measurement is required; for example, with full pose measurement $S = 12$ and $C = 6$ (Masory et al., 1993).

Nahvi et al. (1994) calibrated a spherical shoulder joint (first introduced by Kurtz and Hayward 1992), driven redundantly by four prismatic legs (Figure 4). For this system, $M = 3$ and $S = 4$, so that $C = 1$. Hence self-calibration is possible. This is one advantage of the redundant design (another is increased workspace); without the extra leg and the sensing it provides, one would have $C = 0$. Nahvi et al. (1994) formulated four equations per pose by comparing one sensor reading against the three others; it follows that three of these equations must have been redundant.

Hollerbach and Lokhorst (1995) calibrated a commercial hand controller, which can be considered a platform driven by three rotary legs. In each arm, there is an unsensed spherical wrist and sensed upper arm joints ($S = 9$). Given that $M = 6$, therefore $C = 3$.

Some papers calibrate serial-link arms, but employ external linkages which can be considered as instrumented prismatic legs. Hence the resulting systems can be considered as two-legged platforms. Goswami et al. (1993) employed a ball bar with linear extension measured by an LVDT. This ball bar can be viewed the same as a leg in a Stewart platform. Here $S_J = 1$ and $D_J = 0$, and so $C = 1$. An equivalent setup was the single-wire potentiometer employed by Driels and Swayze (1994).

Driels (1993) employed a ball bar with fixed length. The length constraint on the ball bar yields one calibration equation for each pose; here $S_J = 0$ and $D_J = 1$, and so $C = 1$. This method is equivalent to the use of the measured extendable ball bar of Goswami et al. (1993) above in terms of yielding one equation per pose, and again illustrates the equivalence of endpoint measurements and constraints. There may be other reasons for preferring one method over another. An advantage of the fixed length ball bar is the lack of instrumentation; an advantage of the variable length ball bar is the automatic adjustment to particular endpoint positions and a larger set of reachable poses.

4.2 Laser Limbs

Laser interferometers have been successfully used as external metrology systems, or have themselves been the subjects for kinematic calibration. When multiple beams are employed, a parallel linkage can be considered to be formed if the laser beams are considered as kinematic linkages (Figure 2). Depending on which joints of these "legs" are measured, different calibration procedures result.

$S_J = 3$: Sometimes the pan-tilt mirror angles are sensed, as well as the linear displacement, as part of the calibration. The laser tracker is then serving as a 3D point measurement source, like many other metrology systems such as camera-based triangulation systems.

$S_J = 5$: Additionally, a measured steerable pan-tilt mirror on the end effector can be employed instead of a retroreflector (Lau et al. 1985).

$S_J = 1$: If a retroreflector is employed and pan-tilt measurements are not provided, then only linear displacement is sensed. Something roughly equivalent was done by Tang and Liu (1993), who employed a single laser displacement meter. Their method required the laser to be positioned roughly perpendicular to the flat surfaces of a stack of blocks and that manipulator displacements be made roughly perpendicularly. The requirement for perpendicularity obviates the need for a scanning head or retroflector.

A problem with laser interferometers is that they provide only incremental distance measurements; an extra calibration procedure is required to establish absolute lengths. The Chesapeake Bay Laser System is a 3-beam laser tracking system that provides 3D point measurement of a retroreflector (Mooring et al. 1991); as in the case just discussed, pan-tilt angles of the scanning mirrors are not provided. Zhuang et al. (1992) proposed to calibrate autonomously for absolute lengths by adding a fourth scanning laser interferometer; at the same time relative locations of each tracker are determined.

We now analyze how addition of a fourth tracker permits auto-calibration, through the equivalent kinematic linkage (Figure 5). Three trackers are modeled as 6-DOF prismatic legs as in Figure 2. The fourth tracker is a 3-DOF leg with a solid block at the end instead of a spherical joint; the other trackers attach with spherical joints to this solid block. The mobility $M = 3$ while $S = 4$, hence $C = S - M = 1$. Thus one equation per pose results, and closed-loop calibration is possible. If only 3 trackers were used, then again $M = 3$ but $S = 3$ and $C = 0$, i.e., self-calibration is not possible. In their paper, Zhuang et al. (1992) actually formulated 16 equations per pose, by comparing each sensor reading against combinations of the other 3 sensor readings; our analysis indicates that 15 of these equations are redundant.

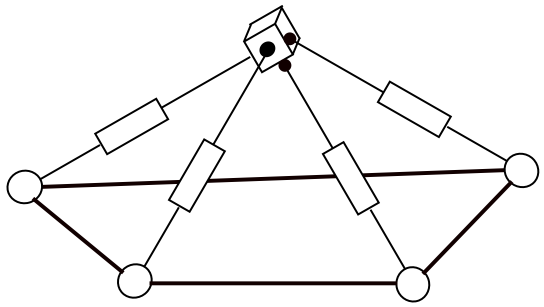

Figure 5: Equivalent linkage for 4-beam laser scanning system.

Newman and Osborn (1993) used a laser to define a line in space, rather than to measure length interferometrically. A retroreflector mounted on the end effector reflects the laser light back to a 4-quadrant detector, whose output is used to servo the manipulator to track the line. For a serial link manipulator, then $D_J = 2$ because orthogonal distance from the line is constrained to be zero, the retroreflector does not constrain orientation, and motion along the line is unconstrained. Since length along the line is not measured, then $S_J = 0$ yielding $C = 2$. In their procedure, Newman and Osborne minimize based on predicted 3D coordinates, which yields one redundant equation.

4.3 Light Limbs

Zhuang et al. (1993) developed a closed-loop procedure for calibration of a robot with a single camera mounted on the end effector. Unlike interferometers, length is not measured, whereas the camera's detector is considered the equivalent of measuring the Hooke joint. A single loop is formed with $S_J = 2$ and $D_J = 0$; hence $C = 2$. In the lens model, radial distortion was parameterized through a quadratic function and identified.

Bennett et al. (1991) showed that an uncalibrated stereo camera system could be simultaneously calibrated with an uncalibrated manipulator. Consider the mechanical linkage equivalent of their system (Figure 3). Two cameras on tripods track a distinguished point on a 6-DOF arm. The rays from each camera to the tracked point are modeled as prismatic legs. Each tripod is presumed to have a sensed rotation about the azimuth axis. For this system, it turns out that $M = 8$ and $S = 12$; hence $C = 4$ and self-calibration is possible. It follows that two of the six equations used in Bennett et al. (1991) must have been redundant.

5 The Role of Input Noise

The closed-loop viewpoint of calibration methods leads to an implicit kinematic equation (1), in which there is no longer a notion of input (joint angles) or output (endpoint pose) variables. Moreover, joint angle measurement error or noise is often significant relative to endpoint measurement error or noise. The approach of ordinary least squares, applied iteratively to the linearized kinematic equations by practically all previous investigators, is therefore problematical. Ordinary least squares minimizes the error in the output variables while assuming there is no noise in the input variables. It is known that the presence of input noise in ordinary least squares leads to bias errors in the parameter estimates (Norton 1986).

For kinematic calibration methods employing passive endpoint constraints, such as rigid attachment, then there can be virtually no endpoint measurement error (except for any attachment backlash) and hence error sources are dominated by joint angle measurement errors. Hence the use of ordinary least squares is inappropriate. Similar comments can be made about other calibration problems, such as inertial parameter estimation, where the error in joint velocities or accelerations is usually significant relative to joint torque error and where the use of ordinary least squares is dominant.

5.1 Orthogonal Distance Regression

A very few papers in robotics have recently begun to address input noise, which we survey. We first examine related developments in the statistics and numerical analysis communities, which have proposed methodologies to handle input noise in linear or nonlinear parameter estimation problems. In the statistics community, the approach is termed by some as orthogonal distance regression, while in the numerical analysis community the approach is called total least squares.

As a simple example, consider the linear equation $y = ax$, where only the slope a is to be determined. If the uncertainties in the input/output variables are σ_x and σ_y, then the weighted normal distances from points (x_i, y_i) to the line are minimized:

$$\chi^2 = \sum_{i=1}^{P} \frac{(y_i - ax_i)^2}{\sigma_y^2 + a^2\sigma_x^2} \tag{8}$$

which is a χ^2 statistic (Bevington 1992; Press et al. 1992). To solve this equation, Press et al. (1992) proposed an iterative nonlinear optimization procedure.

The formulation and solution of equations like (8) have appeared under various names and guises over the years, including total least squares (Van Huffel and Vandewalle 1991), orthogonal distance regression (Boggs et al. 1987), or errors-in-variables regression (Fuller 1987). One common application is to fit a plane to a set of measured 3D points; all 3 components of measured position have noise. For example, this problem arises when measuring multiple points on an end effector and establishing a coordinate system (e.g., An et al. 1988). Another example is circle point analysis, where a plane is to be fit to the circle of points generated by moving a single joint (Mooring et al. 1991). Total least squares solves such equations analytically using singular value decomposition, making unnecessary the iterative solution proposed in Press et al. (1992).

Even more pertinent to kinematic calibration, nonlinear versions of the total least squares problem have been developed. As another simple example, suppose we are now trying to fit a scalar function $y = f(x, a)$ by adjusting some parameters a (Boggs et al. 1987). Assuming again equivalent error in x and y measurements, we should minimize the Euclidean distances from the measurements to the fitted curve f (Figure 6).

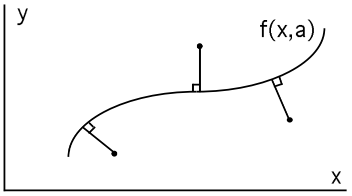

Figure 6: Fitting a curve $y = f(x, a)$ with both input and output errors.

Consider open-loop calibration of serial manipulators, where an explicit kinematic equation results:

$$\mathbf{y}^i = \mathbf{f}^i(\mathbf{x}^i, \boldsymbol{\phi}) \tag{9}$$

where we now separate the endpoint pose measurements $\mathbf{y}^i$ from the joint angle measurements $\mathbf{x}^i$. This forward kinematics function is again stacked for all poses:

$$\mathbf{y} = \mathbf{f}(\mathbf{x}, \boldsymbol{\phi}) \tag{10}$$

where $\mathbf{y} = (\mathbf{y}^1, \ldots, \mathbf{y}^p)$, etc. This equation is rewritten to reflect both the input $\Delta\mathbf{x}$ and output $\Delta\mathbf{y}$ measurement errors:

$$\mathbf{y} - \Delta\mathbf{y} = \mathbf{f}(\mathbf{x} - \Delta\mathbf{x}, \boldsymbol{\phi}) \tag{11}$$

Let the covariances of the output and input variables be $\mathbf{R} = \mathbf{E}(\Delta\mathbf{y}\Delta\mathbf{y}^T)$ and $\mathbf{P} = \mathbf{E}(\Delta\mathbf{x}\Delta\mathbf{x}^T)$, where $\mathbf{E}$ is the expectation operator. Then minimize the weighted orthogonal squared distances from the measurements $(\mathbf{y}, \mathbf{x})$ to the multidimensional surface represented by $\mathbf{y} = \boldsymbol{f}(\mathbf{x}, \boldsymbol{\phi})$:

$$\min_{\boldsymbol{\phi}, \Delta\mathbf{y}, \Delta\mathbf{x}} \chi^2 = \Delta\mathbf{y}^T\mathbf{R}^{-1}\Delta\mathbf{y} + \Delta\mathbf{x}^T\mathbf{P}^{-1}\Delta\mathbf{x} \tag{12}$$

subject to (11). The solution proceeds by substituting (11) into (12) to eliminate $\Delta\mathbf{y}$, and an unconstrained optimization problem results which is solved as usual by linearization and iteration (Schwetlick and Tiller 1985).

Such an approach for robot calibration was taken by Zak et al. (1994). Consider the linearization of (9):

$$\Delta\mathbf{y}^i = \mathbf{J}^i\boldsymbol{\phi} \tag{13}$$

where $\mathbf{J}^i$ is the Jacobians of $\mathbf{f}^i$ with regard to the joint angle sensors $\mathbf{x}$ at pose i. Zak et al. augmented the output variance in this linearized equation with the transformed input variance as follows:

$$\tilde{\mathbf{R}} = \mathbf{R} + \mathbf{J}\mathbf{P}\mathbf{J}^T \tag{14}$$

where $\mathbf{J} = \mathrm{diag}(\mathbf{J}^1, \ldots, \mathbf{J}^P)$ is a block-diagonal matrix. This weighting equation is the generalization of the weighting in (8). Zak et al. (1994) then apply weighted least squares iteratively, at each step treating $\mathbf{J}$ (which contains the unknown parameters) as a constant matrix based on the current estimates, and obtaining the weighted least squares estimate with the modified $\tilde{\mathbf{R}}$.

5.2 Implicit Loop Method

Renders et al. (1991) and Wampler et al. (1995) proposed methods for kinematic calibration equivalent to nonlinear total least squares, with the addition of *a priori* parameter estimates as in damped least squares. Following the development in (Wampler et al. 1995), an implicit equation results from the unifying view of open-loop kinematic calibration methods as closed-loop methods (2). Again, all measurements, whether from joint angle sensors or endpoint sensors, are grouped together.

Let us suppose that the true measurements are $\mathbf{x} = \mathbf{x}_0 + \mathbf{x}_e$, where $\mathbf{x}_0$ is the measurement and $\mathbf{x}_e$ is the measurement error. Similarly, factor the true parameter values into $\boldsymbol{\phi} = \boldsymbol{\phi_0} + \boldsymbol{\phi_e}$, where $\boldsymbol{\phi_0}$ is our initial estimate and $\boldsymbol{\phi_e}$ is the estimation error. Because $\mathbf{x}_0$ and $\boldsymbol{\phi_0}$ are known, they are incorporated as constants into the loop closure equation (2), which is then a function

$$\mathbf{f}(\mathbf{x}_e, \boldsymbol{\phi}_e) = \mathbf{0} \tag{15}$$

The maximum likelihood estimate minimizes

$$\chi^2 = \mathbf{x}_e^T\mathbf{R}^{-1}\mathbf{x}_e + \boldsymbol{\phi}_e^T\mathbf{M}^{-1}\boldsymbol{\phi}_e \tag{16}$$

subject to (15), where $E(\mathbf{x}_e\mathbf{x}_e^T) = \mathbf{R}$ and $\boldsymbol{E}(\boldsymbol{\phi_e}\boldsymbol{\phi_e^T}) = \mathbf{M}$.

This minimization problem is solved by linearization of the constraints and iteration. Let the scaled variables $\mathbf{y}$ and $\mathbf{q}$ be defined via $\mathbf{x}_e = \mathbf{R}^{1/2}\mathbf{y}$ and $\boldsymbol{\phi}_e = \mathbf{M}^{1/2}\mathbf{q}$, where the superscript 1/2 means the symmetric square root. Iterate from an initial guess $\mathbf{y} = \mathbf{0}$ and $\mathbf{q} = \mathbf{0}$ to find corrections $\Delta\mathbf{y}$ and $\Delta\mathbf{q}$ to minimize

$$\chi^2 = (\mathbf{y} + \Delta\mathbf{y})^T(\mathbf{y} + \Delta\mathbf{y}) + (\mathbf{q} + \Delta\mathbf{q})^T(\mathbf{q} + \Delta\mathbf{q}) \tag{17}$$

subject to the linearized constraints

$$\begin{aligned} -\mathbf{f}'(\mathbf{y},\mathbf{q}) &= \frac{\partial\mathbf{f}'}{\partial\mathbf{y}}(\mathbf{y},\mathbf{q})\Delta\mathbf{y} + \frac{\partial\mathbf{f}'}{\partial\mathbf{q}}(\mathbf{y},\mathbf{q})\Delta\mathbf{q} \\ &\equiv \mathbf{J}_y\Delta\mathbf{y} + \mathbf{J}_q\Delta\mathbf{q} \end{aligned} \tag{18}$$

Compute the QR-decomposition $\mathbf{Q}\tilde{\mathbf{R}} = \mathbf{J}_y^T$ (this is actually done individually for each pose) and define

$$\mathbf{D} = \tilde{\mathbf{R}}^{-T}\mathbf{J}_y, \quad \mathbf{E} = \mathbf{Q}^T\mathbf{y} - \tilde{\mathbf{R}}^{-T}\mathbf{f}(\mathbf{y},\mathbf{q}) \tag{19}$$

The variables $\Delta\mathbf{y}$ are eliminated and the step in $\mathbf{q}$ found from:

$$\begin{bmatrix} \mathbf{D} \\ \mathbf{I} \end{bmatrix} \Delta\mathbf{q} = \begin{bmatrix} \mathbf{E} \\ -\mathbf{q} \end{bmatrix} \tag{20}$$

and the updated error estimates are

$$\mathbf{y} + \Delta\mathbf{y} = \mathbf{Q}(\mathbf{E} - \mathbf{D}\mathbf{q}) \tag{21}$$

Covariance matrices are scaled *post facto* based on the value of χ^2.

Because the loop closure equation (15) is an implicit function of all measurements, Wampler et al. (1995) coined the term *Implicit Loop Method.* Whereas in nonlinear total least squares (12) the output errors could be directly eliminated by using the explicit constraint equation, for the implicit loop method the linearization of the implicit constraint equation was required for this elimination. The earlier approach of Renders et al. (1991) deals only with open-loop calibration of serial arms; the resulting explicit constraint equation is incorporated using Lagrange multipliers rather than using variable elimination as in (12). Like Zak et al. (1992), linearization is at nominal values, whereas in the Implicit Loop Method the unknown parameters from the linearization also come into play.

6 Discussion

This paper has proposed the calibration index, which indicates how many equations per pose result for a calibration method. Use of this index can help one to understand how a particular calibration method relates to others, and what the tradeoffs are in fashioning a calibration method. To get enough equations for calibration, one needs sufficient numbers of poses. With a higher calibration index, a particular calibration method would require fewer poses. On the other hand, more complex metrology systems could be required to get more measured components of pose if open-loop calibration is used.

It should be be emphasized that the calibration index is only a first-order characterization of calibration methods. Even if two putative methods have the same calibration index, other considerations might dictate a preference of one over the other. Perhaps an external metrology system is not available, in which closed-loop methods would be perferred. On the other hand, closed-loop methods typically constrain pose set selection more than open-loop calibration, so one has to analyze observability of parameters carefully.

With the view that kinematic calibration methods are all closed-loop methods, an implicit loop closure equation results that doesn't distinguish input from output variables. The issue then arises of handling input noise as well as output noise, which is scarcely recognized in the robotics calibration literature. Orthogonal distance regression has been developed to handle such problems in the statistics literature. A related development is the implicit loop method of Wampler et al. (1995), which also incorporates *a priori* parameter estimates.

Acknowledgments. Support for this research was provided by the NSERC NCE IRIS II Project AMD-5, and by NSF Grant MIP-9508588.

References

An, C.H., Atkeson, C.G., and Hollerbach, J.M. 1988. *Model-Based Control of a Robot Manipulator.* Cambridge, MA: MIT Press.

Bennett, D.J., and Hollerbach, J.M. 1991. Autonomous calibration of single-loop closed kinematic chains formed by manipulators with passive endpoint constraints. *IEEE Trans. Robotics and Automation.* 7: 597-606.

Bennett, D.J., Hollerbach, J.M., and Geiger, D. 1991. Autonomous robot calibration for hand-eye coordination. *Int. J. Robotics Research.* 10: 550-559.

Bevington, P.R., and Robinson, D.K. 1992. *Data Reduction and Error Analysis for the Physical Sciences*. N.Y.: McGraw-Hill.

Boggs, P.T., Byrd, R.H., and Schnabel, R.B. 1987. A stable and efficient algorithm for nonlinear orthogonal distance regression. *SIAM J. Sci. Stat. Comput.*. 8: 1052-1078.

Craig, J.J. 1993 (November). Calibration of industrial robots. *Proc. 24th Intl. Symp. on Industrial Robots*. Tokyo: pp. 889-893.

Driels, M.R. 1993. Using passive end-point motion constraints to calibrate robot manipulators. *J. Dynamic Systems, Meas., Control*. 115: 560-565.

Driels, M.R., and Swayze, W.E. 1994. Automated partial pose measurement system for manipulator calibration experiments. *IEEE Trans. Robotics and Automation*. 10: 430-440.

Fuller, W.A. 1987. *Measurement Error Models*. NY: John Wiley & Sons.

Giugovaz, L., and Hollerbach, J.M. 1994 (Sept. 12-16). Closed-loop kinematic calibration of the Sarcos Dextrous Arm. *Proc. IEEE/RSJ Intl. Conf. on Intelligent Robots and Systems*. Munich, Germany: pp. 329-334.

Goswami, A., Quaid, A., and Peshkin, M. 1993. Identifying robot parameters using partial pose information. *IEEE Control Systems*. 13(5): 6-14.

Hollerbach, J.M. 1993 (Oct. 2-5). Advances in robot calibration. *Robotics Research: The Sixth International Symposium*. Hidden Valley, PA: pp. 319-326.

Hollerbach, J.M., and Lokhorst, D. 1995. Closed-loop kinematic calibration of the RSI 6-DOF hand controler. *IEEE Trans. Robotics and Automation*. 11: 352-359.

Kurtz, R., and Hayward, V. 1992. Multiple-goal kinematic optimization of a parallel spherical mechanism with actuator redundancy. *IEEE Trans. Robotics and Automation*. 8: 644-651.

Lau, K., Hocken, R., and Haynes, L. 1985. Robot performance measurements using automatic laser tracking techniques. *Robotics & Computer-Integrated Manufacturing*. 2: 227-236.

Masory, O., Wang, J., and Zhuang, H. 1993 (May 2-7). On the accuracy of a Stewart platform - part II Kinematic calibration and compensation. *IEEE Intl. Conf. Robotics and Automation*. Atlanta: pp. 1:725-731.

McCarthy, J.M. 1990. *Introduction to Theoretical Kinematics*. Cambridge, MA: The MIT Press.

Mooring, B.W., Roth, Z.S., and Driels, M.R. 1991. *Fundamentals of Manipulator Calibration*. NY: Wiley Interscience.

Nahvi, A., Hollerbach, J.M., and Hayward, V. 1994 (May 8-13). Closed-loop kinematic calibration of a parallel-drive shoulder joint. *Proc. IEEE Intl. Conf. Robotics and Automation*. San Diego: pp. 407-412.

Newman, W.S., and Osborn, D.W. 1993 (May 2-7). A new method for kinematic parameter calibration via laser line tracking. *IEEE Intl. Conf. Robotics and Automation*. Atlanta: pp. 2:160-165.

Norton, J.P. 1986. *An Introduction to Identification*. London: Academic Press.

Press, W.H., Teukolsky, S.A., Vetterling, W.T., and Flannery, B.P. 1992. *Numerical Recipes in C*. Cambridge, UK: Cambridge Univ. Press.

Renders, J.-M., Rossignol, E., Becquet, M., and Hanus, R. 1991. Kinematic calibration and geometrical parameter identification for robots. *IEEE Trans. Robotics and Automation*. 7: 721-732.

Schwetlick, H., and Tiller, V. 1985. Numerical methods for estimating parameters in nonlinear models with errors in variables. *Technometrics*. 27: 17-24.

Tang, G.-R., and Liu, L.-S. 1993. Robot calibration using a single laser displacement meter. *Mechatronics*. 3: 503-516.

Van Huffel, S., and Vandewalle, J. 1991. *The Total Least Squares Problem: Computational Aspects and Analysis*. Philadelphia: SIAM.

Vincze, M., Prenninger, J.P., and Gander, H. 1994. A laser tracking system to measure position and orientation of robot end effectors under motion. *Intl. J. Robotics Research*. 13: 305-314.

Wampler, C., and Arai, T. 1992 (Sept. 24-26). Calibration of robots having kinematic closed loops using non-linear least-squares estimation. *Proc. IFTOMM Symp.*. Nagoya, Japan: pp. 1:153-158.

Wampler, C.W., Hollerbach, J.M., and Arai, T. 1995. An Implicit Loop Method for kinematic calibration and its application to closed-chain mechanisms. *IEEE Trans. Robotics and Automation.* 11: 710-724.

Whitney, D.E., Lozinski, C.A., and Rourke, J.M. 1986. Industrial robot forward calibration method and results. *ASME J. Dynamic Systems, Meas., Control.* 108: 1-8.

Zak, G., Benhabib, B., Fenton, R.G., and Saban, I. 1994. Application of the weighted least squares parameter estimation method for robot calibration. *J. Mechanical Design.* 116: 890-893.

Zhong, X.-L., and Lewis, J.M. 1995 (May 21-26). A new method for autonomous robot calibration. *IEEE Intl. Conf. Robotics and Automation.* Nagoya: pp. 1790-1795.

Zhuang, H., Li, B., Roth, Z.S., and Xie, X. 1992. Self-calibration and mirror center offset elimination of a multi-beam laser tracking system. *Robotics and Autonomous Systems.* 9: 255-269.

Zhuang, H., Wang, K., and Roth, Z.S. 1995. Simultaneous calibration of a robot and a hand-mounted camera. *IEEE Trans. Robotics and Automation.* 11: 649-660.

Zhuang, H., Wang, L., and Roth, Z.S. 1993 (May 2-7). Simultaneous calibration of a robot and a hand-mounted camera. *IEEE Intl. Conf. Robotics and Automation.* Atlanta: pp. 2:149-154.